

## Overview of the CMD-3 recent results

**A E Ryzhenenkov**<sup>1,2</sup>, **R R Akhmetshin**<sup>1,2</sup>, **A N Amirkhanov**<sup>1,2</sup>, **A V Anisenkov**<sup>1,2</sup>, **V M Aulchenko**<sup>1,2</sup>, **V Sh Banzarov**<sup>1</sup>, **N S Bashtovoy**<sup>1</sup>, **D E Berkaev**<sup>1,2</sup>, **A E Bondar**<sup>1,2</sup>, **A V Bragin**<sup>1</sup>, **S I Eidelman**<sup>1,2,6</sup>, **D A Epifanov**<sup>1,2</sup>, **L B Epshteyn**<sup>1,2,3</sup>, **A L Erofeev**<sup>1,2</sup>, **G V Fedotovich**<sup>1,2</sup>, **S E Gayazov**<sup>1,2</sup>, **F J Grancagnolo**<sup>4</sup>, **A A Grebenuk**<sup>1,2</sup>, **S S Gribanov**<sup>1,2</sup>, **D N Grigoriev**<sup>1,2,3</sup>, **F V Ignatov**<sup>1</sup>, **V L Ivanov**<sup>1,2</sup>, **S V Karpov**<sup>1</sup>, **A S Kasaev**<sup>1</sup>, **V F Kazanin**<sup>1,2</sup>, **I A Koop**<sup>1,2</sup>, **A A Korobov**<sup>1,2</sup>, **A N Kozyrev**<sup>1,3</sup>, **E A Kozyrev**<sup>1,2</sup>, **P P Krovovny**<sup>1,2</sup>, **A E Kuzmenko**<sup>1</sup>, **A S Kuzmin**<sup>1,2</sup>, **I B Logashenko**<sup>1,2</sup>, **P A Lukin**<sup>1,2</sup>, **A P Lysenko**<sup>1</sup>, **K Yu Mikhailov**<sup>1</sup>, **V S Okhapkin**<sup>1</sup>, **E A Perevedentsev**<sup>1,2</sup>, **Yu N Pestov**<sup>1</sup>, **A S Popov**<sup>1,2</sup>, **G P Razuvaev**<sup>1,2</sup>, **A A Ruban**<sup>1</sup>, **N M Ryskulov**<sup>1</sup>, **A V Semenov**<sup>1,2</sup>, **Yu M Shatunov**<sup>1</sup>, **V E Shebalin**<sup>1,2,7</sup>, **D N Shemyakin**<sup>1,2</sup>, **B A Schwartz**<sup>1,2</sup>, **D B Schwartz**<sup>1,2</sup>, **A L Sibidanov**<sup>1,5</sup>, **E P Solodov**<sup>1,2</sup>, **M V Timoshenko**<sup>1</sup>, **A A Talyshев**<sup>1,2</sup>, **S S Tolmachev**<sup>1</sup>, **A I Vorobiov**<sup>1,2</sup>, **Yu V Yudin**<sup>1,2</sup>

<sup>1</sup>Budker Institute of Nuclear Physics, SB RAS, Novosibirsk, 630090, Russia

<sup>2</sup>Novosibirsk State University, Novosibirsk, 630090, Russia

<sup>3</sup>Novosibirsk State Technical University, Novosibirsk, 630092, Russia

<sup>4</sup>Istituto Nazionale di Fisica Nucleare, Sezione di Lecce, Lecce, Italy

<sup>5</sup>University of Victoria, Victoria, BC, Canada V8W 3P6

<sup>6</sup>Lebedev Physical Institute RAS, Moscow, 119333, Russia

<sup>7</sup>University of Hawaii, Honolulu, Hawaii 96822, USA

E-mail: [tem\\_mc@mail.ru](mailto:tem_mc@mail.ru)

**Abstract.** The CMD-3 detector started data taking at the electron-positron collider VEPP-2000 in December 2010 with a goal to collect about  $1 \text{ fb}^{-1}$ . The collected data sample corresponds to an integrated luminosity of  $200 \text{ pb}^{-1}$  in the center-of-mass energy range from 0.32 up to 2 GeV. This paper reports recent results on the hadronic cross sections measurements with the CMD-3 detector.

### 1. Introduction

The electron-positron collider VEPP-2000 [1] is designed to provide a luminosity of up to  $10^{32} \text{ cm}^{-2} \text{ s}^{-1}$  at a maximum center-of-mass (c.m.) energy of  $\sqrt{s} = 2 \text{ GeV}$ . Two detectors, CMD-3 [2] and SND [3], are installed in the two interaction regions of the collider. Both detectors have good energy and angular resolutions for charged particles and photons.

The main goal of CMD-3 is a study of exclusive modes of  $e^+e^- \rightarrow \text{hadrons}$  in the c.m. energy range below 2 GeV. The CMD-3 results provide an important input for the calculation of the hadronic contribution to the muon anomalous magnetic moment and will help reducing the uncertainty of its SM prediction. The physics program also includes studies of intermediate

dynamics of hadron processes, studies of known and searches for new vector mesons, studies of  $p\bar{p}$  and  $n\bar{n}$  production cross sections near threshold and searches for exotic hadrons.

## 2. CMD-3 detector and dataset

The Cryogenic Magnetic Detector [2], CMD-3, is a general-purpose detector. The cylindrical drift chamber (DC) measures the coordinates, angles and momenta of charged particles. The resolution along the beam axis is  $\sim 2$  mm as measured by charge division along the wires. The proportional wire Z-chamber mounted outside the DC provides z-coordinate measurement of the tracks. The resulting z-coordinate resolution is  $\sim 500$   $\mu\text{m}$ . The calorimeter consists of three subsystems: the endcap BGO calorimeter with a depth of  $13.4X_0$  is placed on both sides of the DC flanges; the barrel part, which is placed outside the superconducting solenoid with a 1.3 T magnetic field ( $0.13X_0$ ). The barrel consists of two systems: an inner Liquid Xenon calorimeter ( $5.4X_0$ ) and a calorimeter based on CsI crystals with a depth of  $8.1X_0$ . The analog strip information from the LXe calorimeter allows to measure coordinates of the photon conversion point with a precision of about 1-2 mm. The detector is surrounded by the muon range system.

The collected integrated luminosity is  $200 \text{ pb}^{-1}$  per detector, with about  $65 \text{ pb}^{-1}$  from a scan below the  $\phi(1020)$  meson region and  $135 \text{ pb}^{-1}$  above the  $\phi(1020)$ , including  $14 \text{ pb}^{-1}$  of data at nucleon-antinucleon production threshold region.

Since 2017 operation went on with the upgraded injection facility that allowed an increase of the average luminosity by a factor of three.

The integrated luminosity was measured by counting  $e^+e^- \rightarrow e^+e^-$  and  $e^+e^- \rightarrow \gamma\gamma$  events, allowing additional photons in the final state. The systematic uncertainty of the luminosity measurement at high energies is estimated to be 1% [4].

The beam energy measurement system [5] has been installed and commissioned in 2012. The system allows to continuously monitor the beam energy with a relative precision better than  $10^{-4}$ , using Compton backscattering of laser photons by the electron beam.

## 3. $e^+e^- \rightarrow \pi^+\pi^-$ cross section measurement

One of the main goals of CMD-3 is to reduce the systematic uncertainty on the cross section for two-pion production to a level lower than 0.5%, which corresponds to  $\sim 0.35$  ppm uncertainty in the muon anomalous magnetic moment.

Two energy scans below 1 GeV for the  $\pi^+\pi^-$  measurement were performed in 2013 and 2018. The collected data sample corresponds to an integrated luminosity of  $63 \text{ pb}^{-1}$ . Energy scans above 1 GeV were performed in 2011, 2012, 2017 and 2019. The collected data sample for the c.m. energy range above 1 GeV corresponds to about  $135 \text{ pb}^{-1}$  of integrated luminosity. The collected data sample has the same or better statistical precision for the cross section measurements than was achieved by other experiments.

Separation of collinear  $e/\mu/\pi$  events is performed using either the information on the energy deposition in the calorimeter or on particle momenta measured in the drift chamber. Pions are well separated from electrons by momentum in the c.m. energy range up to 0.9 GeV, while muons are separated from other particles up to  $\sqrt{S} \leq 0.66$  GeV. The separation using energy deposition works better at higher energies and becomes less robust at lower energies.

In both methods the number of muons can be extracted by event separation or can be fixed according to QED prediction. Determination of the number of different particles is done by minimization of the binned likelihood function, where two dimensional PDF functions are constructed in different ways for each type of information.

The current estimated systematic uncertainty is about 0.65% at the  $\rho$ -peak and up to 0.9% at lowest points for momentum-based approach and up to 1.5% for the energy deposition technique.

Preliminary results of  $e^+e^- \rightarrow \pi^+\pi^-$  cross section measurement were published in [6].

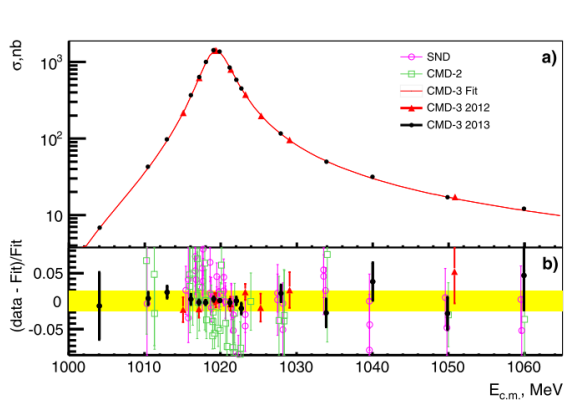


**Figure 1.** (a)  $e^+e^- \rightarrow K_SK_L$  cross section measured in the CMD-3 experiment. (b) Relative difference between the data and fit.

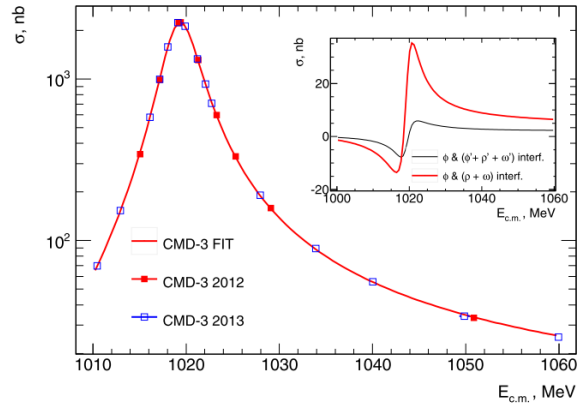


**Figure 2.**  $e^+e^- \rightarrow K^+K^-$  cross section measured by CMD-3. The inset shows the contributions of the  $\rho$  and  $\omega$  intermediate states (red curve) and higher excitations (black curve).

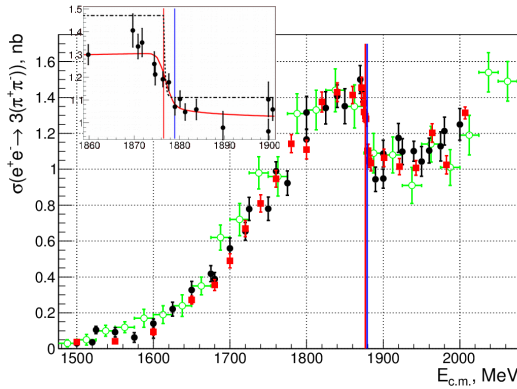


**Figure 3.** The  $e^+e^- \rightarrow 3(\pi^+\pi^-)$  cross section, measured by the CMD-3 in the 2017 runs (red), in 2011-2012 (black), and by BaBar (green). The inset shows the visible cross section with the fit. The lines show  $NN$  thresholds.

#### 4. $e^+e^- \rightarrow K^+K^-, K_SK_L$ channels

A precise measurement of  $e^+e^- \rightarrow K_SK_L$  cross section, dominated by the contribution of the  $\phi(1020)$  and  $\phi(1680)$  resonances, is required to improve our knowledge of the hadronic contributions to muon ( $g - 2$ ). The result of the  $e^+e^- \rightarrow K_SK_L$  cross section measurement [7] is shown in Fig.1. This is the most precise measurement of this cross section with reached 1.8% systematic uncertainty.

The  $e^+e^- \rightarrow K^+K^-$  cross section was measured [8] at the  $\phi(1020)$  energy range to 2% systematic accuracy (Fig.2). The CMD-3 result is in good agreement with isospin symmetry: comparing to the recent CMD-3 measurement  $e^+e^- \rightarrow K_SK_L$ , the ratio of coupling constants taking into account the Coulomb factor is:  $g_{\phi K^+K^-}/g_{\phi K_SK_L}/\sqrt{Z(m_\phi^2)} = 0.990 \pm 0.017$ .

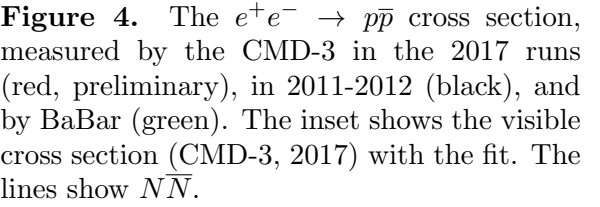


**Figure 4.** The  $e^+e^- \rightarrow pp$  cross section, measured by the CMD-3 in the 2017 runs (red, preliminary), in 2011-2012 (black), and by BaBar (green). The inset shows the visible cross section (CMD-3, 2017) with the fit. The lines show  $NN$ .

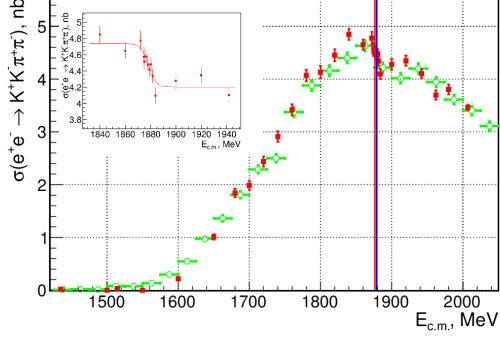


**Figure 5.** The  $e^+e^- \rightarrow K^+K^-\pi^+\pi^-$  Born cross section measured with the CMD-3 detector in the 2017 run (red points). The results of the BaBar measurements are shown by green open circles. The inset shows the visible cross section with the fit described in the text. The vertical lines show the  $NN$  thresholds.

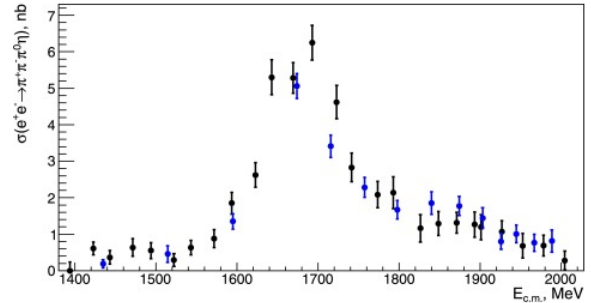


**Figure 6.** The  $e^+e^- \rightarrow \pi^+\pi^-\pi^0\eta$  cross section obtained with the CMD-3 detector. Black and blue colors represent the 2011 and 2012 data, respectively.

## 5. Study of multihadron production at $NN$ threshold

An integrated luminosity of about  $14 \text{ pb}^{-1}$  has been collected in a scan at the  $NN$  threshold with a step comparable with the beam energy spread of 1.2 MeV.

A detailed study of the  $NN$  threshold region confirms a fast drop in the  $e^+e^- \rightarrow 3(\pi^+\pi^-)$  cross section observed previously. The cross section, measured with CMD-3, is shown in Fig.5. The final results for the 2011-2012 data were published in [9].

The results for the  $e^+e^- \rightarrow p\bar{p}$  cross section near threshold are shown in Fig.4. The measured  $e^+e^- \rightarrow p\bar{p}$  cross section and  $G_E/G_M$  ratio for the 2011-2012 data were published in [10].

The analysis of the  $e^+e^- \rightarrow K^+K^-\pi^+\pi^-$  process was described in detail in [11]. The cross section obtained from the new data is shown in Fig.5. The energy position of the drop in the  $e^+e^- \rightarrow K^+K^-\pi^+\pi^-$  cross sections, observed for the first time, is consistent with the  $n\bar{n}$  production threshold, while that for the  $e^+e^- \rightarrow 3(\pi^+\pi^-)$  reaction is close to the  $p\bar{p}$  threshold.

## 6. Study of the process $e^+e^- \rightarrow \pi^+\pi^-\pi^0\eta$

CMD-3 performed the first measurement of  $e^+e^- \rightarrow \pi^+\pi^-\pi^0\eta$  ( $\eta \rightarrow \gamma\gamma$ ) cross section in the c.m. energy range from 1.394 to 2.007 GeV. The obtained cross section is presented in Fig. 6. The production dynamics is dominated by the  $\omega(782)\eta$  and  $\phi(1020)\eta$  intermediate states in the lower energy range, and by the  $a_0(980)\rho(770)$  intermediate state at higher energies. The systematic uncertainty was estimated to be 15%. Results of  $e^+e^- \rightarrow \pi^+\pi^-\pi^0\eta$  study are published in [12].

## 7. Study of the process $e^+e^- \rightarrow K^+K^-\eta$

The analysis of the process  $e^+e^- \rightarrow K^+K^-\eta$  was based on an integrated luminosity of  $59 \text{ pb}^{-1}$  collected by the CMD-3 detector in 2011, 2012 and 2017 in the c.m. energy range from 1.59 to 2.01 GeV. In the production of the  $K^+K^-\eta$  final state we observed the contribution of the  $\phi(1020)\eta$  intermediate state only. The  $K/\pi$  separation was performed with the use of  $f_{K/\pi}(p, dE/dx)$  functions [11], representing the probability density for charged  $K/\pi$  with the momentum  $p$  to produce the energy loss  $dE/dx$  in the DC. The cross section of  $e^+e^- \rightarrow \phi(1020)\eta$  process is shown in Fig.7 along with the BaBar results. The systematic uncertainty on the

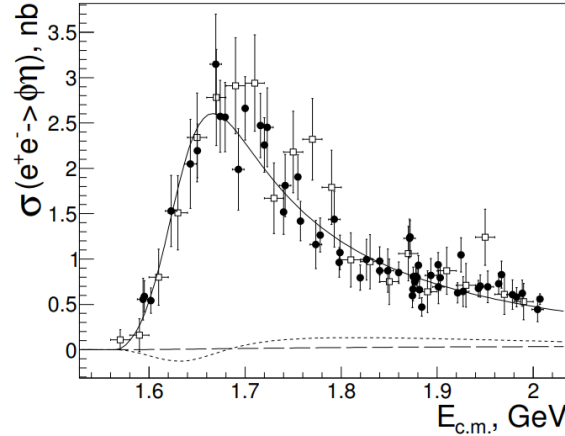


**Figure 7.** BaBar (open squares) and CMD-3 (filled circles) results for the measurement of the  $e^+e^- \rightarrow \phi\eta$  cross section. The overall fit of CMD-3 data (the solid curve), nonresonant part (the dashed curve) and the interference part of the fit (the dotted curve) are shown.

cross section measurement was estimated to be 5.1%. Via the cross section approximation the  $\phi(1680)$ -meson parameters have been determined and the results are published in [13].

## 8. Conclusion

The VEPP-2000 collider successfully operates with a goal of collecting  $\sim 1 \text{ fb}^{-1}$  and providing new precise results on hadron physics. The collected data correspond to an integrated luminosity of  $200 \text{ pb}^{-1}$ . The collected data sample has the same or better statistical precision for the hadronic cross sections than the one achieved in previous experiments.

## Acknowledgements

We thank the VEPP-2000 personnel for excellent machine operation. The work was supported by the Russian Foundation for Basic Research grants RFBR 17-02-00847-a (in part, related to the  $e^+e^- \rightarrow \pi^+\pi^-$  cross section measurement) and RFBR 17-02-00897-a (in part, related to the  $e^+e^- \rightarrow K^+K^-\eta$  process study).

## References

- [1] Koop I A *et al.*, Nucl. Phys. B, Proc. Suppl. **181**, 371 (2008)
- [2] Khazin B I *et al.*, Nucl. Phys. B, Proc. Suppl. **181-182**, 376 (2008)
- [3] Achasov M N *et al.*, Nucl. Instrum. Meth. **A598**, 31 (2009)
- [4] Ryzhenenkov A E *et al.*, EPJ Web Conf. **212**, (2019) 04011
- [5] Abakumova E V *et al.*, Phys. Rev. Lett. **110**, 140402 (2013)
- [6] Ignatov F V *et al.*, EPJ Web Conf. **218**, (2019) 02006
- [7] Kozyrev E A *et al.*, Phys. Lett. **B760**, (2016) 314
- [8] Kozyrev E A *et al.*, Phys. Lett. **B779**, (2018) 64-71
- [9] Akhmetshin R R *et al.*, Phys. Lett. **B723**, 82 (2013)
- [10] Akhmetshin R R *et al.*, Phys. Lett. **B759**, 634 (2016)
- [11] Shemyakin D N *et al.*, Phys. Lett. **B756**, (2016) 153-160
- [12] Akhmetshin R R *et al.*, Phys. Lett. **B773**, (2017) 150-158
- [13] Ivanov V L *et al.*, Phys. Lett. **B798**, (2019) 134946